

## **SIMULATION OF STRONG GROUND MOTION AND RESPONSE OF THE HADDO WHARF SITE AT PORT BLAIR DUE TO SUMATRA EARTHQUAKE**

**Boominathan ADIMOOLAM<sup>1</sup>, Raghudeep BETHAPUDI<sup>2</sup> and Uma Maheswari RAJU<sup>3</sup>**

### **ABSTRACT**

Historically, the Sumatra region has been a very active tectonic zone and has experienced several devastating earthquakes that are controlled by the tectonic processes in a convergent plate margin along the Sumatra trench. On 26<sup>th</sup> December, an earthquake of magnitude  $M_w$  9.1 struck off the northwest coast of Sumatra in the Indonesian Archipelago. Due to this devastating earthquake, an extensive seismic damage to engineering infrastructure has been occurred in northern and north-western Sumatra. The Haddo Wharf site at Port Blair in Andaman & Nicobar Islands (India) is also subjected to severe damage. After this severe earthquake/tsunami, formation of a lengthy crack on the surface and eruption of the soil was found. But the real cause of the ground failure whether due to earthquake or tsunami is not established. Therefore, the present study has been focused on the assessment of intensity of ground shaking and its effect on the ground during Sumatra earthquake.

Due to unavailability of strong recorded ground motion, simulation of ground motion has been carried out using the stochastic method proposed by Boore (2003). The Ground motion spectrum is generated by Atkinson & Boore model (1995). The source and earthquake scenario parameters have been obtained from Sorenson et al. (2006). Then the response of site under simulated ground motion has been studied by conducting one dimensional ground response analysis. Liquefaction analysis was carried out by cyclic stress approach.

Based on the above study bed rock acceleration and ground surface acceleration of the site have been established. The presence of loose silty sand and soft clay deposits of about 21 m thickness caused the significant amplification of the ground. The liquefaction analysis indicates the occurrence of liquefaction of the loose silty sand deposit which caused the settlement of the filledup ground observed after earthquake.

**Keywords:** Sumatra earthquake, source model, ground motion simulation, site response, liquefaction

### **INTRODUCTION**

On 26<sup>th</sup> December 2004, an earthquake of magnitude  $M_w$  9.1 at 3.316°N, 95.854°E struck off the northwest coast of Sumatra in the Indonesian Archipelago at 06:29 hrs (Indian Standard Time). It is mainly due to subduction of Indo-Australian plate beneath the Burma microplate which is a part of Eurasian plate making it the most powerful in the world in the last 40 years. The Indian plate has been moving north – east at a rate of approximately 60 mm per year, subducting under the overriding Burma microplate.

<sup>1</sup>Professor, Department of Civil Engineering, Indian Institute of Technology Madras, Chennai, India, Email: [boomi@iitm.ac.in](mailto:boomi@iitm.ac.in)

<sup>2</sup>Formerly Under Graduate Student, Department of Civil Engineering, Indian Institute of Technology Madras, Chennai, India

<sup>3</sup>Research Scholar, Department of Civil Engineering, Indian Institute of Technology Madras, Chennai, India

The epicenter of the quake is 155 km west of Sumatra and about 255 km south east of Banda Aceh, Indonesia. The focal depth is at a depth of 30 km and the estimated ruptured fault length is 1300 km. Strong ground shaking and Tsunami accompanying the earthquake caused widespread damage to port and harbour facilities at Port Blair, Andaman & Nicobar Islands. As a consequence of movement of Indo-Australian plate and the Burma micro-plate (part of Eurasian plate), the Andaman Islands experienced uplift and subsidence at different places. The Sumatra earthquake resulted in tilting of the plate along the EW direction with a tilt towards the east. The relative subsidence of the Burma Plate along an East–West strike is about  $1.2 \pm 0.2$  m. In this perspective it becomes very important to study the hazards caused by the earthquake.

Due to the Sumatra earthquake, the ground failure was observed at the container yard at Haddo Wharf site at Port Blair which is shown in Figure 1. The container yard is the unpaved well compacted fill of about 4 m thick overlying on the soft natural ground close to the berthing structure. The formation of a lengthy crack on the surface and eruption of the soil at the surface of the unpaved container yard observed after the earthquake are shown in Figure 1(a) and 1(b) respectively. The number of cracks formed at the container yard and settlement with respect to the berthing structure are shown in Figure 1(c) and 1(d) respectively. But the real cause of the ground failure, whether due to earthquake or tsunami is not established. Therefore, the present study has been focused on the assessment of intensity of ground shaking and its effect on the Haddo Wharf site at port Blair due to Sumatra earthquake.

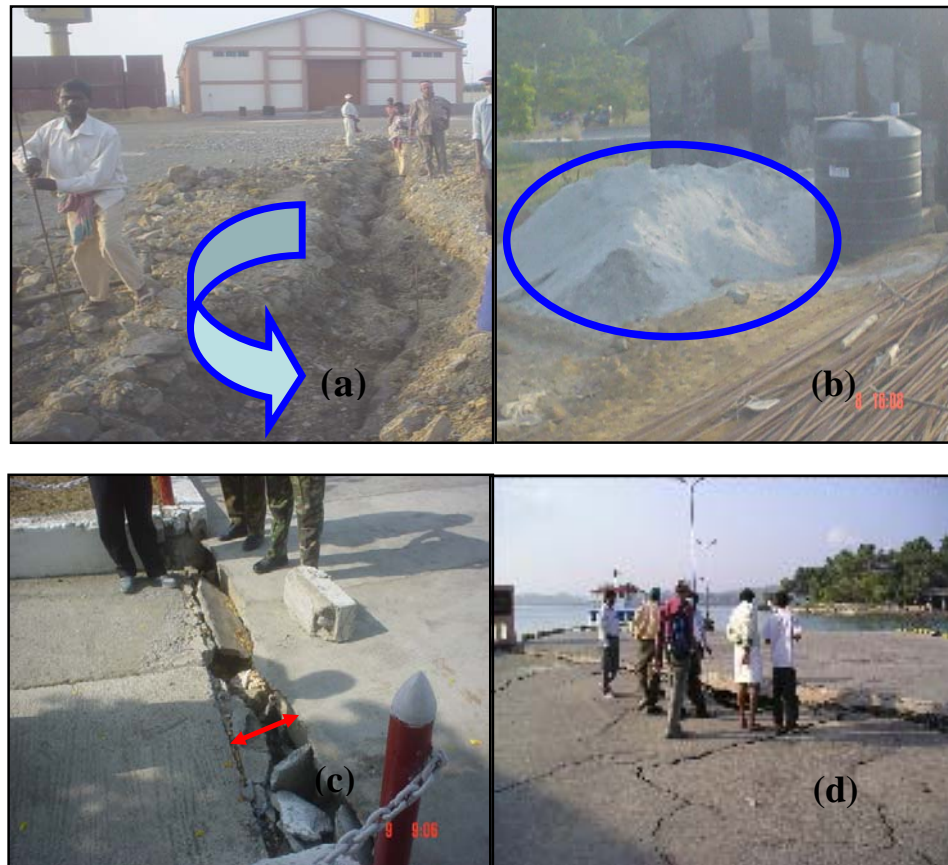


**Figure 1: Ground failures at unpaved container yard, Haddo Wharf site, Port Blair (Andaman & Nicobar Islands) during Sumatra earthquake**

**(a) Cracks through which eruption of liquefied silty sand occurred**

**(b) Liquefied silty sand (c) Settlement of container yard (d) Series of cracks and settlement**

Due to unavailability of strong recorded ground motion, simulation of ground motion has been carried out using the stochastic method proposed by Boore (2003). The Ground motion spectrum is generated by Atkinson & Boore model (1995). The source and earthquake scenario parameters have been

obtained from Sorenson et al. (2006). Then the response of the site under simulated ground motion has been studied by conducting one dimensional ground response analysis. Liquefaction analysis also carried out using cyclic stress approach.

## **GROUND MOTION MODELING**

A simple and powerful method for simulating ground motions is to combine parametric or functional descriptions of the ground motion's amplitude spectrum with a random phase spectrum modified such that the motion is distributed over a duration related to the earthquake magnitude and to the distance from the source. This method of simulating ground motions often goes by the name "Stochastic method." It is particularly useful for simulating the higher-frequency ground motions of most interest to engineers (generally,  $f > 0.1$  Hz), and it is widely used to predict ground motions for regions of the world in which recordings of motion from potentially damaging earthquakes are not available. One of the essential characteristics of the method is that it distills what is known about the various factors affecting ground motions (source, path, and site) into simple functional forms.

## **SOURCE MODEL FOR SUMATRA - ANDAMAN EARTHQUAKE**

The shallow angle of subduction allows considerable amount of stress to accumulate and hence generates large earthquakes. The plate boundary runs parallel to the Sunda Trench. In the north, the boundary is more or less aligned towards the N-S direction but as we go down towards the south (at around  $10^{\circ}\text{N}$ ), the boundary starts to get inclined towards the East and thus produces an arc like structure called the Sunda Arc. Due to N-NE movement of the plate, the earthquake distribution (amount of earthquake epicenters) in the southern region is higher compared to that of the northern region since it gives rise to considerable dip slip movement. The dip of the subducting plate is relatively low ( $\approx 10^{\circ}$ ) at shallower depth ( $< 30$  km). With increasing depth, the dip becomes steeper ( $\approx 40-45^{\circ}$ ). The maximum depths of the earthquakes range between 150-300 km and gradually increase from 150 km in the north ( $\approx 13^{\circ}\text{N}$ ) to almost 300 km in the south ( $\approx 4^{\circ}\text{N}$ ).

The earthquake rupture initiated at around  $3^{\circ}\text{N}$  latitude along the Sunda trench at a depth of about 30 km. The rupture occurred in three stages (Sorenson et al., 2006). The Sumatra segment consisting of the first 420 km, starting from the rupture initiation point, where the slip was upto 20 m and with an average rupture velocity of 3 km/s. The Nicobar segment consisting of the next 325 km, where the slip was within 5 m and with an average rupture velocity of 2.5 km/s. The Andaman segment consisting of 570 km, where the slip was within 2 m, and the whole rupture took place from 600 s upto 3500 s. The seismic moment of the Sumatra and the Nicobar segments were  $6.5 \times 10^{22}$  N-m and  $3.0 \times 10^{22}$  N-m respectively. The total energy released from the rupture was  $4.3 \times 10^{18}$  J. A simplified version of the Sorenson et al model (2006) is shown in Figure 2. This model has been used as the source model. In this case the source consists of a number of asperities, which are divided into subfaults assumed to be point sources. Point sources are summed using the empirical Green's function method of Irikura (1986). The most of the models based on the stochastic method are fundamentally point-source models. Although it is true that near and intermediate-field terms are lacking, in most applications the frequencies are high enough that the far-field terms dominate, even if the site is near the fault. Furthermore, the effects of a finite-fault averaged over a number of sites distributed around the fault (to average over radiation pattern and directivity effects) can be captured in several ways: 1) using the closest distance to faulting as the source-to-site distance 2) using a two-corner source spectrum 3) allowing the geometrical spreading to be magnitude dependent.

The length and the width of the fault are taken as 750 km and 150 km respectively. The seismic moment is assumed as  $6.5 \times 10^{22}$  N-m, which corresponds to the seismic moment released during the rupture of Sumatra and Nicobar segments. The entire fault plane is assumed to rupture uniformly

producing the same stress drop across the entire area. The stress drop is taken as the average stress drop. (Sorenson et al, 2006). The scenario earthquake parameters are tabulated in Table 1.

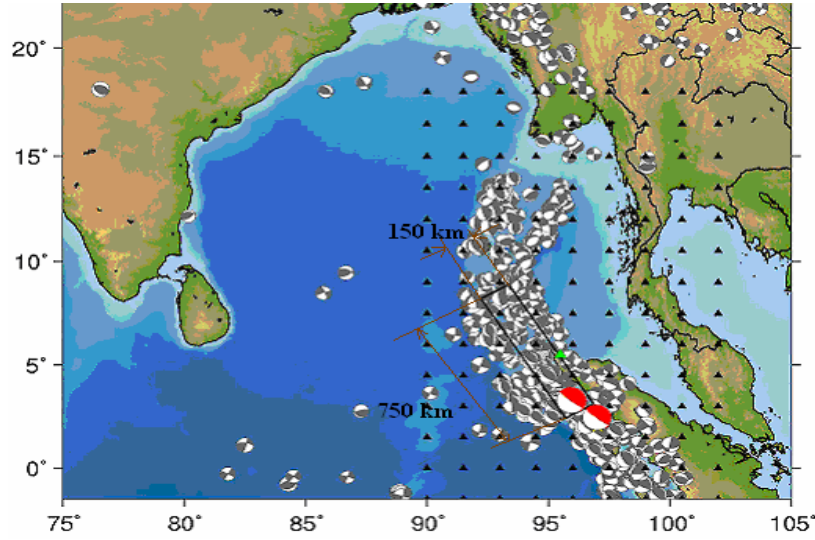


**Figure 2: Source model (Sorenson et al, 2006)**

**Table 1: Scenario earthquake parameters**

Input parameters	Value
Seismic Moment, $M_0$	$6.5 \times 10^{22}$ Nm
Average asperity stress drop, $\Delta\sigma$	60 Bars
Shear wave Velocity of the bedrock (site), $v_s$	1100 m/s
Density of the bedrock, $\rho_s$	2600 kg/m <sup>3</sup>
Shortest distance between source and site, R	315 km
Duration of Strong Ground Motion, $T_{gm}$	21.7 s
Q (frequency dependent quality factor)	$100 \times f^{0.8}$
$f_{max}$ (cutoff frequency)	10 Hz
$C_Q$ (Rupture velocity)	$2.5 \pm 0.5$ km/s

### **SIMULATION OF STRONG GROUND MOTION**

For simulating the strong ground motion, the Stochastic Method is used. The method assumes that the far-field accelerations on an elastic half space are band-limited, finite-duration, white Gaussian noise, and that the source spectra are described by a single corner-frequency model whose corner frequency depends on earthquake size. The ground spectrum  $Y(M_0, R, f)$  is conveniently broken into several simple functions – the Earthquake source (E); the Path (P); the Site (G) and the instrument or type of motion (I).

$$Y(M_0, R, f) = E(M_0, f) \times P(R, f) \times G(f) \times I(f) \quad (1)$$

where,  $M_0$  is the seismic moment, R is the shortest distance from the fault to the site and f is the frequency. Atkinson & Boore model (1995) has been used to obtain the ground motion spectrum. The process of simulation of strong ground motion is depicted as a flowchart in Figure 3.

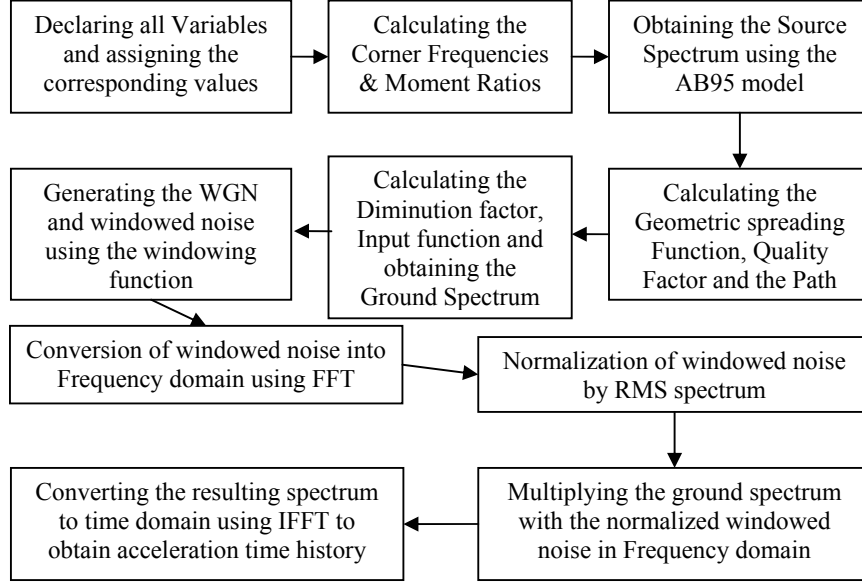


**Figure 3: Flow chart showing the structure of the MATLAB program**

### Source spectrum

The source spectrum  $E$  is obtained by the following equation specifying both the shape and the amplitude as a function of the earthquake size.

$$E(M_0, f) = C \times M_0 \times S_a(M_0, f) \times S_b(M_0, f) \quad (2)$$

By adopting the source spectrum model AB95, the above equation for source spectrum is rewritten considering the seismic moment dependence of the above factors  $S_a$  in terms of corner frequencies  $f_a$  and  $f_b$ :

$$E(M_0, f) = CM_0 \left\{ \frac{1 - \varepsilon}{1 + \left( \frac{f}{f_a} \right)^2} + \frac{\varepsilon}{1 + \left( \frac{f}{f_b} \right)^2} \right\} \quad (3)$$

where  $C$  is the constant given by  $C = \frac{\langle R_{\Theta\Phi} \rangle VF}{4 \pi \rho_s \beta_s R_0}$  (4)

Here,  $\langle R_{\Theta\Phi} \rangle$  accounts for the radiation pattern ( $\approx 0.55$ ),  $V$  represents the partition of total shear wave energy into horizontal components ( $= 0.707$ ),  $F$  accounts the effect of free surface ( $\approx 2$ ) and  $\rho_s$  and  $\beta_s$  are the density and shear wave velocity of the bedrock.  $R_0$  is a reference distance and usually taken as 1km. The corner frequencies  $f_a$  and  $f_b$  are obtained from the seismic moment using the following relation

$$\ln(f_a) = 2.41 - 0.533 M_0 \quad (5)$$

$$\ln(f_b) = 1.43 - 0.188 M_0 \quad (6)$$

The Source duration is evaluated as  $0.5/f_a$

### Path spectrum

The path effects are represented by simple functions that describe the geometric spreading function, attenuation (intrinsic and scattering attenuation). The simplified path effect  $P$  is given by the multiplication of the geometrical spreading and  $Q$  functions:

$$P = Z(R) \exp \left\{ \frac{-\pi R f}{Q(f) C_Q} \right\} \quad (7)$$

The effects of the path can be represented by simple functions that account for geometrical spreading, attenuation (combining intrinsic and scattering attenuation), and the general increase of duration with distance due to wave propagation and scattering. The relation between distance and geometrical spreading function  $Z(R)$  is given by the following function

$$Z(R) = \frac{1}{70} \sqrt{\frac{130}{R}} \quad (8)$$

and  $Q(f)$  is the Frequency Dependent Quality Factor which is given by the following equation

$$Q(f) = 100 f^{0.8} \quad (9)$$

The path duration function of  $0.05R$  is calculated from Atkinson and Boore (1995)

### Site Spectrum

The attenuation or diminution operator  $D(f)$  accounts for the path-independent loss of high-frequency in the ground motions. A simple multiplicative filter can account for the diminution of the high frequency motions. Here  $f_{\max}$  is 10 Hz. The diminution factor is calculated based on the following equation

$$D(f) = \{1 + (f/10)^8\}^{-0.5} \quad (10)$$

### Type of ground motion

The particular type of ground motion resulting from the simulation is controlled by the filter  $I(f)$ . If ground motion is desired, then

$$I = -(2\pi f)^n \quad (11)$$

where,  $i = (-1)^{0.5}$ .  $n = 0, 1, 2$  for ground displacement, velocity or acceleration respectively.

### Windowed WGN

A time domain simulation is carried out to get the actual Fourier amplitude spectrum. A White Gaussian Noise (WGN) is produced and windowed off using a windowing function given below

$$W(t; \varepsilon, \eta, t_\eta) = a (t/t_\eta)^b \times \exp \{-c (t/t_\eta)\} \quad (12)$$

where,

$$a = \{\exp(1)/e\}^b$$

$$b = -(\varepsilon \ln \eta) / [1 + \varepsilon (\ln \varepsilon - 1)]$$

$$c = b/\varepsilon$$

$$t_\eta = f_{T_{gm}} \times T_{gm}$$

Boore suggested the values of  $\varepsilon$  and  $\eta$  to be 0.2 and 0.05 respectively and  $f_{T_{gm}} = 2$  based on Saragoni and Hart (1974). The windowed WGN is converted to frequency domain and normalized by its root mean square amplitude. The entire process of obtaining WGN is shown in Figure 4. Then the ground motion spectrum shown in Figure 5 is multiplied with the normalized windowed noise to get the Fourier amplitude spectrum as shown in Figure 6.

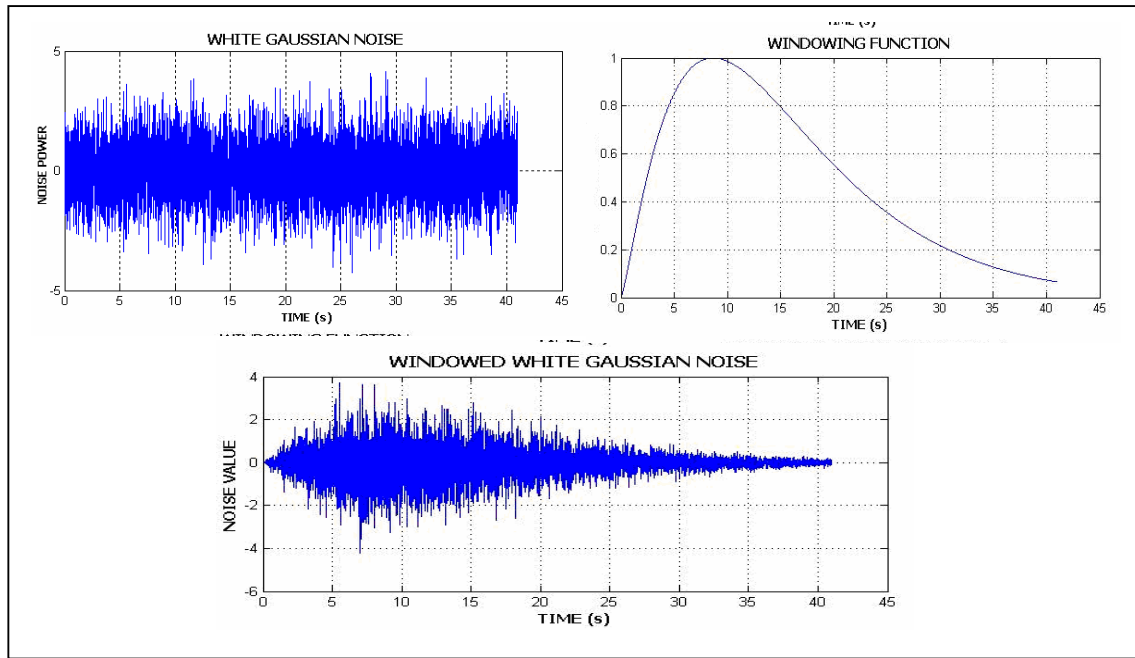


**Figure 4: Process of obtaining a windowed WGN**

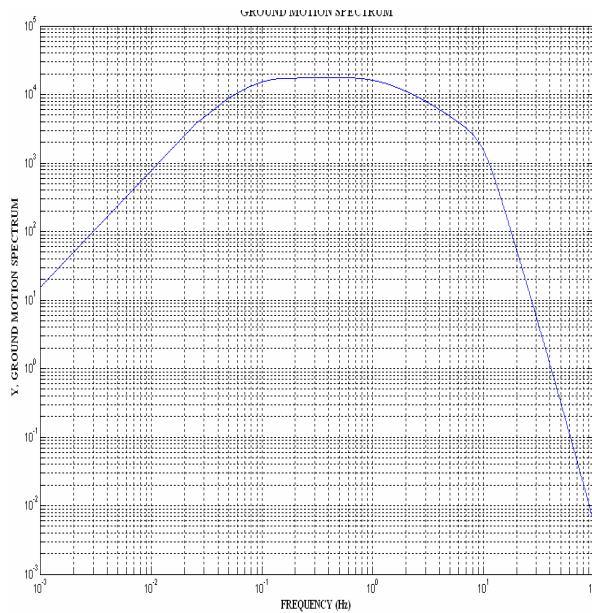


**Figure 5: Ground Motion Spectrum**

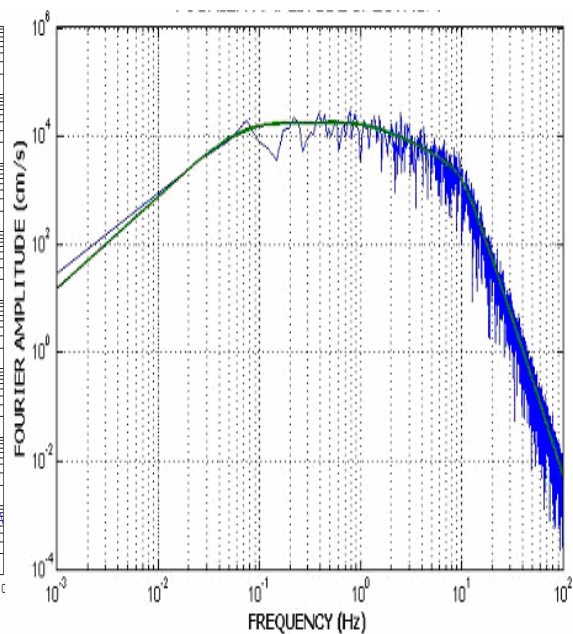


**Figure 6: Fourier Amplitude Spectrum with randomness**

### **SIMULATED GROUND MOTION**

A sample simulated acceleration time history is shown in Figure 7. This site is located at a distance of 315 km from the source and is in this respect expected to experience strong shaking. This has also been confirmed by eyewitness (e.g. the on-line intensity map of USGS [http://pasadena.wr.usgs.gov/shake/ous/STORE/Xslav\\_04/ciim\\_display.html](http://pasadena.wr.usgs.gov/shake/ous/STORE/Xslav_04/ciim_display.html)).



The maximum intensity of the earthquake shaking along the A & N Is. is placed at VII on the MSK or the MMI Intensity scale. Applying empirical relations between peak ground motion and intensity gives correspondingly a PGA of approximately 0.18 g to 0.34 g (Murphy and O'Brien, 1977). Our simulations indicate ground motions reaching acceleration levels of 0.154 g. A comparison of the ground motion values obtained by modeling and based on the intensities shows that we expect site amplifications in the order of a factor of 1.2 - 2.3. This is a reasonable estimate, considering that we are dealing with strong ground motion in an area where local site effects are expected to be significant. Another important information given by the simulated waveforms is the duration of the ground shaking which has a significant impact on the resulting damage. From the waveforms, it is seen that shaking in Andaman & Nicobar lasted for approximately 15 s.

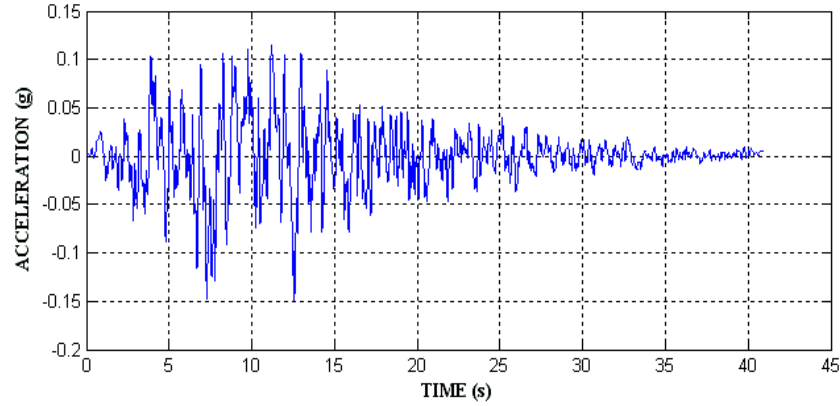


**Figure 7: Simulated acceleration time history**

## **SITE RESPONSE ANALYSIS**

### **Description of soil profile**

Soil investigation carried out before earthquake at the Haddo Wharf site shows that the top soil below natural ground consists of 1.5 m thick silty clay layer with SPT N- value in the range of 5 to 8. It is followed by 20 m thick silty sand with SPT N - value in the range of 12 to 20. The hard rock occurs at a depth of 21.5 m from the ground surface. Ground water was encountered at a depth of 3 m below the ground level.

### **Site effects**

One-dimensional ground response analysis of the site was carried out by equivalent linear approach using SHAKE 91 program (Idriss et al., 1992). For site specific response analysis, it is recommended to use shearwave velocity measured in the field and modulus reduction curve obtained from the laboratory cyclic tests. However, due to non availability of the above parameters, the shearwave velocity estimated from the empirical relationship available between SPT-N value and shearwave velocity and the standard modulus reduction curves are used. Among the available empirical relationships, the following equation proposed by Japan Road Association (2002) is widely used in the practice and the same is adopted in the present study.

$$\text{For clay: } V_s = 100 \times (N)^{1/3} \quad (13)$$

$$\text{For sand: } V_s = 80 \times (N)^{1/3} \quad (14)$$

The estimated average shearwave velocity of soil within 20 m was found to be around 670 m/s. The standard modulus reduction and damping curves for clay and sandy soils proposed by Seed and Idriss (1970) was used in the present study. The simulated ground motion was used as the input motion with peak acceleration of 0.154 g and bracketed duration of 15s for ground response analysis. The results of ground response analysis are presented in Figures 8 to 10. The variation of maximum acceleration with the depth as shown in Figure 8 indicates that the increase of PGA at the surface is about two times higher than at the bed rock. Figure 9 shows the variation of amplitude ratio i.e. ratio of Fourier



amplitude at the surface to the bed rock. It can be easily noticed from Figure 9 that the significant amplification occurs only at the frequency of about 2.0 Hz. The response spectra obtained from ground response analysis for 5% damping is shown in Figure 10. This figure shows the occurrence of very high value of spectral acceleration of above 1.0 g at the range of period from 0.8 s to 1.2 s.

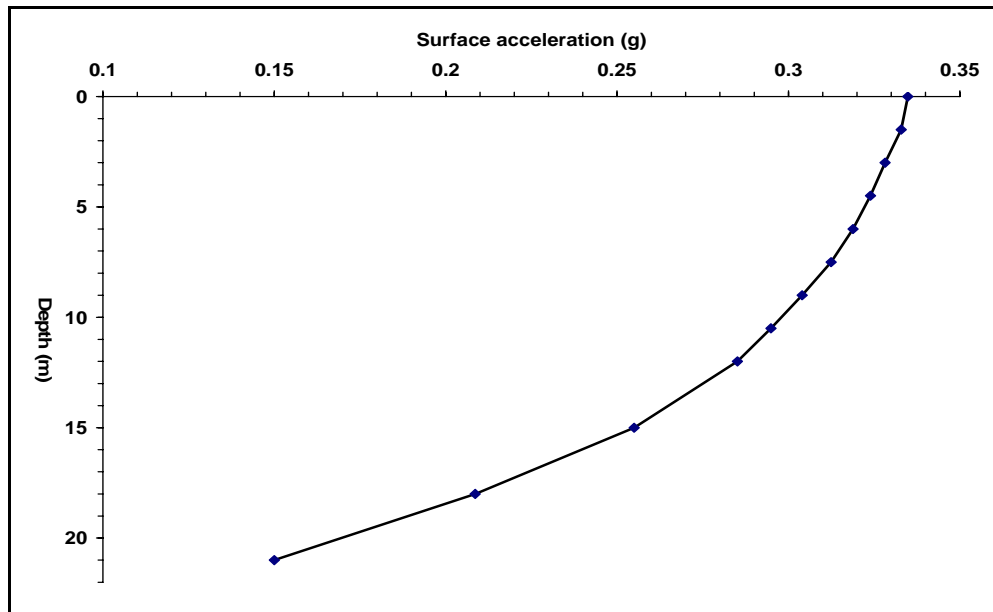


Figure 8: Variation of surface acceleration with depth for typical Borehole

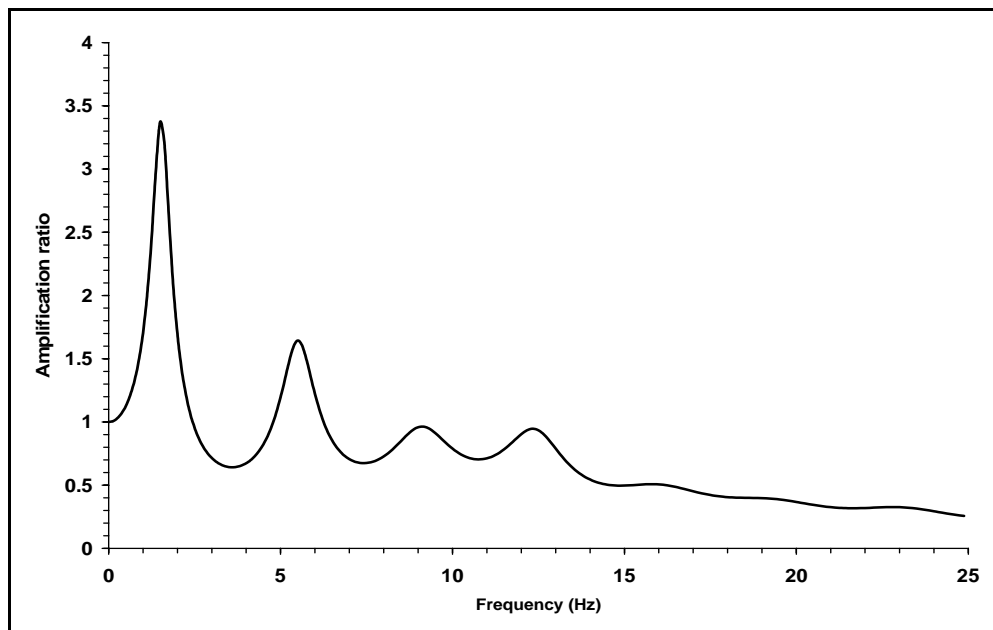
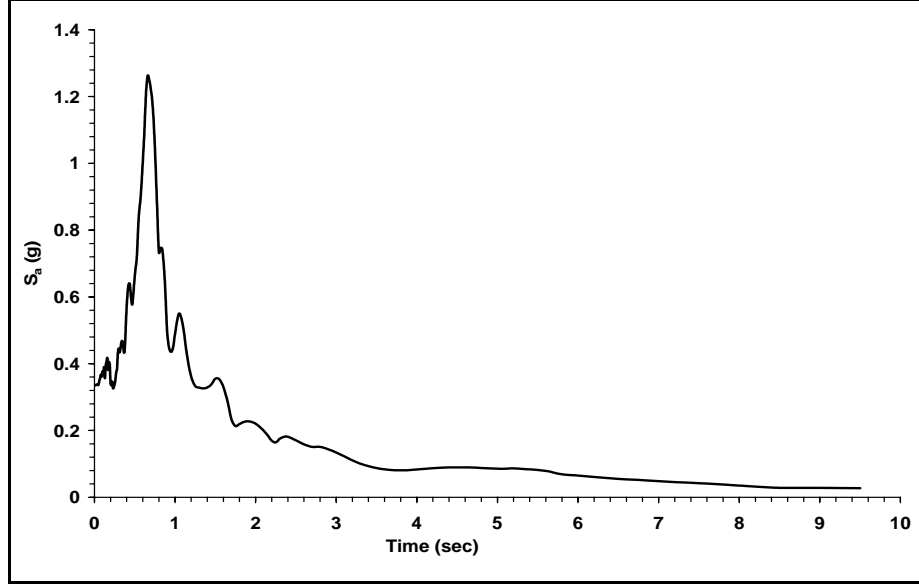


Figure 9: Amplification ratio plot



**Figure 10: Response spectrum plot**

### LIQUEFACTION ANALYSIS

The most widely used method for evaluating the initiation of liquefaction is the Cyclic Stress Approach (e.g. Seed and Idriss, 1971; Youd and Idriss, 2001; Idriss and Boulanger, 2006). In this approach, the earthquake-induced loading, expressed in terms of cyclic shear stress is compared with the liquefaction resistance of the soil, also expressed in terms of cyclic shear stress. At locations where the loading exceeds the resistance, liquefaction is expected to occur. With this approach the factor of safety against liquefaction is evaluated by comparison of level of cyclic stress ratio (CSR) induced by the earthquake with the level of cyclic stress ratio required to initiate liquefaction (CRR).

The cyclic shear stress ratio induced by the earthquake is calculated using the following equation (Idriss and Boulanger, 2006).

$$(CSR)_{M=7.5, \sigma=1} = 0.65 * \left( \frac{\sigma_{vo} a_{max}}{\sigma'_{vo}} \right) \frac{r_d}{MSF K_\sigma} \quad (15)$$

where  $a_{max}$  is the peak surface ground acceleration obtained from the ground response analysis,  $\sigma_{vo}$  is the total vertical stress,  $\sigma'_{vo}$  is the effective stress,  $r_d$  is the value of a stress reduction factor at the depth of interest and  $K_\sigma$  is the overburden correction factor. The stress reduction factor is calculated using the modified equation

$$\begin{aligned} \ln(r_d) &= \alpha(z) + \beta(z) M \\ \alpha(z) &= -1.012 - 1.126 \sin(z/11.73 + 5.133) \\ \beta(z) &= 0.106 + 0.118 \sin(z/11.28 + 5.142) \end{aligned} \quad (16)$$

In which  $M$  is the moment magnitude,  $z$  is the depth of interest in meters. Theses equations are applicable to a depth of  $z \leq 34$  m.

The magnitude scaling factor,  $MSF$  has been used to adjust the induced CSR during earthquake magnitude  $M$  to an equivalent CSR for an earthquake magnitude,  $M = 7.5$  and it is calculated using the following equation

$$MSF = 6.9 \exp(-M/4) - 0.058 \quad (17)$$

The cyclic shear resistance ratio (CRR) was estimated using a modified CRR –  $(N_1)_{60}$  boundary chart proposed by Idriss and Boulanger (2006) as shown in Figure 10. The factor of safety against liquefaction is evaluated as the ratio of CRR to CSR.

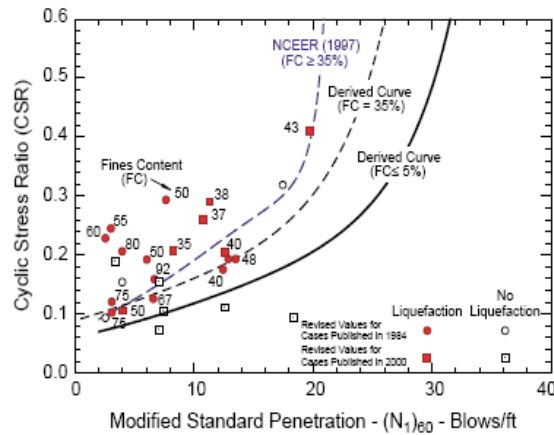


**Figure 10: Modified CRR –  $(N_1)_{60}$  Boundary Chart**

The liquefaction analysis carried out for the site up to a depth of 21 m for moment magnitude of  $M_w$  9.1 and peak ground surface acceleration of 0.34 g shows the factor of safety against liquefaction for the silty sandy deposits is much lower than 1.0 indicating the occurrence of liquefaction of the whole silty sand layer. It would have caused the settlement of the filledup ground, formation of the cracks and eruption of silty sand through cracks.

## SUMMARY AND CONCLUSIONS

During December 2004, Sumatra earthquake of magnitude  $M_w$  9.1 and tsunami the ground failure was observed at Haddo Wharf site, Port Blair of Andaman and Nicobar Islands (INDIA). But the real cause of the ground failure whether due to earthquake or tsunami is not established. Therefore, the present study has been focused on the assessment of intensity of ground shaking and its effect on the ground failure due to Sumatra earthquake. The simulation of ground motion has been carried out using the stochastic method proposed by Boore (2003). Then the response of site under simulated ground motion has been studied by conducting one dimensional ground response analysis. The liquefaction analysis was carried out by cyclic stress approach using SPT N- value. Based on the above study the following conclusions are arrived:

- The maximum PGA at bedrock at the Haddo Wharf site of Port Blair is established as 0.154 g and the duration of bedrock motion is about 15 s.
- Ground response analysis indicates the increase of PGA at the surface is about two times higher than at the bedrock which is well confirmed by the USGS online intensity map for Andaman & Nicobar Islands (USGS).
- The response spectra obtained from the analysis indicates that the spectral acceleration above 1 g corresponds to the periods in the range of 0.8 s to 1.2 s which is the typical range of period for berthing structures constructed in the Port and harbour facilities in Andaman & Nicobar Islands.
- The settlement and eruption of the silty sand through cracks at the container yard site is due to the occurrence of liquefaction of whole silty sand layer.

## REFERENCES

- Atkinson GM. and Boore DM. "Ground motion relations for Eastern North America," Bulletin Seismological Society of America, vol 85, 17-30, 1995
- Boore DM. "Simulation of ground motion using stochastic method", Journal of pure and applied Geophysics, vol. 160, 635-676, 2003
- Idriss, IM and Boulanger RW. "Semi-empirical procedures for evaluating the liquefaction potential during earthquakes," Soil Dynamics and Earthquake Engineering, vol. 26, 115-130, 2006
- Idriss IM and IS Joseph. "User manual for SHAKE 91", 1992
- Irikura K. "Prediction of strong acceleration motion using empirical Green's function," Proceedings of 7<sup>th</sup> Japan Earthquake Engineering Symposium, 151-156, 1986
- Japan Road Association. "Specification and interpretation of bridge design for highway-part V: Resilient Design", 14-15, 1980.
- Kramer SL. "Geotechnical Earthquake Engineering," PHI Inc, 1996.
- Murphy, JR and O'Brien, LJ. "The correlation of peak ground acceleration amplitude with seismic intensity and other physical parameters," Bulletin Seismological Society of America (BSSA), 877-915, 1977.
- Saragoni, GR and Hart, GC. "Simulation of artificial earthquakes", Journal of Earthquake Engineering structural Dynamics, vol 2, 249-267, 1974.
- Seed, HB and Idriss, IM. "Simplified procedure for evaluating the soil liquefaction potential", Journal of Soil Mechanics and Foundation Engineering Division, ASCE, vol 97, 1249-1274, 1971.
- Sorenson MB, Atakan K and Pulido N. "Simulated strong ground motions for the great M9.3 Sumatra Andaman earthquake of 26th Dec 2004," Bulletin of the Seismological Society of America (BSSA), 2006
- Youd, TL. and Idriss, IM. "Liquefaction Resistance of Soils: Summary report from the 1996 NCEER and 1998 NCEER/NSF workshop on evaluation of liquefaction resistance of soils", Journal of Geotechnical and Geo environmental Engineering, ASCE, vol. 127, 297-313, 2001.